Comprehensive Simulation for eVTOL Aircraft-Diagnosing Coupled Airframe-Propulsion Dynamic Instabilities

Felix Brenner
Application Engineer
Gamma Technologies, GmbH
Stuttgart, Germany

Llorenc Foraste Gomez
Product Application Manager
Gamma Technologies, LLC
Chicago, IL, USA

Jan Goericke
Staff Aerospace Engineer
Advanced Rotorcraft Technology
Sunnyvale, CA, USA

Matt Hasbun
Senior Principal Aerospace Engineer
Advanced Rotorcraft Technology
Sunnyvale, CA, USA

ABSTRACT

The design, development, and testing of an eVTOL aircraft requires multiple physics-based simulation applications to address technical challenges and optimize the configuration for stringent mission requirements. While existing rotorcraft simulation and analysis tools are utilized for the analysis of eVTOL configurations, the adoption of an electrified propulsion system introduces new challenges. These tools are tailored for analysis of coupled system dynamics including elastic structures, airloads, and wake interactions, but are lacking capability for detailed electrified drive system dynamics. As a result, the dynamics of the electric drive system are often analyzed separate from the flight and structure dynamics. This can cause important coupled interactions to be overlooked and require costly late-stage design changes. This paper describes and demonstrates the coupling of GT-SUITE, a detailed electric propulsion modeling and analysis tool, with the comprehensive rotorcraft analysis tool, FLIGHTLAB. The objective of coupling these applications was to provide eVTOL analysis capabilities that enable improved designs in terms of mission range, operation capabilities, and flight safety. The successful coupling of these applications was demonstrated with lift and cruise propellers based on the Uber Elevate configuration.

INTRODUCTION

Recently, there has been significant interest and investment in the development of Electric Vertical Take-Off and Landing (eVTOL) vehicles to support Urban Air Mobility (UAM). However, there are several challenges that must be addressed for eVTOL vehicle configurations to achieve their intended UAM mission. These challenges stem from strict airworthiness requirements due to operation over densely populated areas, congested airspace, autonomous or semi-autonomous flight control systems (FCS), and limited aircraft endurance of all-electric aircraft configurations to name a few.

A major consideration of UAM aircraft designers is meeting their mission endurance requirements. This is especially true of eVTOL configurations, with modern batteries providing significantly less energy storage density compared to traditional fossil fuel or hybrid-electric power sources. This constraint on available energy requires careful design of the entire propulsion system, from batteries to rotors, to maximize efficiency. Additionally, integrated full vehicle and propulsion system simulation and optimization of mission power requirements can be used early in the design to mitigate the risks associated with limited energy storage. This optimization can reduce total weight of the components of the electric propulsion system including the sizing of the appropriate heat dissipation components.

To address many of the challenges, eVTOL companies have embraced multi-disciplinary simulation to support aircraft design from conceptual through detailed design. There remain opportunities to combine multi-disciplinary simulation and analysis in a comprehensive modeling approach to address and analyze phenomena which are otherwise difficult to capture before the first flight of the prototype aircraft. Recent publications [1, 2, 3, 4] show that in the design of an eVTOL air vehicle, the airframe and drive systems are conventionally addressed separately. However, this approach can be inefficient and result in less-than-optimal designs for several reasons, including overly conservative design limitations shared between the airframe and drive system teams, time consuming optimization of the combined system with multiple manual iterations between the airframe and drive system teams, and limited capability for modeling transient maneuvers (such as transitioning flight from VTOL to fixed-wing or operations in turbulent urban air) and fault & malfunction scenarios. Furthermore, eVTOL vehicle range has a strong dependency on the full battery-to-rotor propulsion system performance, especially during high power conditions such as take-off and landing. Today, the range of eVTOL configurations is less than 100 miles [5] and is a major consideration in the design process. A coupled airframe and drive system analysis can provide improved prediction of

Presented at the Vertical Flight Society's 78th Annual Forum & Technology Display, Ft. Worth, TX, USA, May 10-12, 2022,

the full vehicle performance, especially in take-off and landing maneuvers, which is critical for component sizing and overall vehicle design due to the high-power demand.

The coupled solution allows the airframe and drive system teams to utilize a consolidated model and eliminates manual iteration while optimizing the airframe and drive system for the following applications:

- Evaluation of the coupled system stability, including through standard mission and edge-of-envelope flight conditions.
- Prediction of coupled transient dynamics and performance of airframe and drive system components, including during fault & malfunction scenarios.
- Component sizing; better-educated choice due to more realistic duty cycles; more accurate battery performance predictions.
- Detailed weight and balance information early in aircraft design and refinement throughout design iterations.
- Mission and flight performance prediction including battery, energy transformation, heat generation, and motor performance with detailed insight into state of battery charge, battery current draw, and heating generation for both batteries and motors.

A multi-physics simulation-led approach to analyzing the combined airframe and drive system has been developed to provide an improved understanding of the airframe/electric-drive system interactional governing physics for electric and hybrid-electric UAM configurations. The capability can facilitate rapid development of an air vehicle while minimizing design costs by providing a better understanding of the full vehicle coupled dynamics in early design iterations.

This paper discusses the implementation of the coupled simulation framework and showcases its capability through the analysis of eVTOL rotor models (FLIGHTLAB) with an integrated propulsion system (GT-SUITE). The rotor structure and aerodynamic model, including unsteady airloads and mutual wake interactions, is coupled with a detailed simulation of the electric propulsion system to address important aspects of an eVTOL design for UAM, such as increased energy efficiency, noise reduction, distributed propulsion and controls, complex fault trees, and simulation-supported aircraft certification. This paper demonstrates the coupled simulation codes and shows results of several multi-physics simulation applications, including rotor dynamic response, battery discharge rates, energy consumption, and heat generation.

IMPLEMENTATION OF AIRFRAME AND DRIVE SYSTEM COUPLED ANALYSIS

A multi-physics simulation approach has been developed to better support simulation and analysis of the coupled dynamics between the rotor/airframe and the electric propulsion systems. The modeling capabilities of FLIGHTLAB, GT-SUITE, and the implementation of the coupled analysis are described below.

FLIGHTLAB ANALYSIS CAPABILITIES

FLIGHTLAB is a well-known finite element, multi-body, selective fidelity modeling and analysis software package supporting modeling and simulation of rotorcraft, fixed-wing aircraft, compound aircraft, drones, flying cars, and experimental aircraft configurations. FLIGHTLAB has been used widely for the modeling, simulation, and analysis of eVTOL aircraft in the past years focusing on the flight mechanical aspects, including mission and flight performance, handling qualities, gust rejection, and operational analyses including fault and malfunction simulation. FLIGHTLAB has been validated for many VTOL applications as discussed in [6]. The electric propulsion system is modeled to the extent required to support the flight mechanical focus. FLIGHTLAB users commonly use the predictions of power required as a decoupled input to their detailed electric propulsion system models constructed in third party or in-house software applications.

GT-SUITE ANALYSIS CAPABILITIES

GT-SUITE is specialized in high level multi-physics modelling and offers a variety of libraries and components to build accurate models of large engineering systems and enables modeling solutions for real-time, HiL/SiL, and control system simulations. Libraries include components to simulate the physics of fluid flow, thermal, mechanical, electrical, magnetic, chemistry, and controls- using a robust non-linear differential equation solver. GT-SUITE has been validated in the past for different electric propulsion designs in the context of UAM[7,8]

IMPLEMENTATION OF THE COUPLED ANALYSIS

GT-SUITE is used to model the electrical, electro-mechanical, and control components of the electric powertrain. The electric powertrain model is used to analyze component performance and component interactions, where the boundary conditions and operation targets are provided by FLIGHTLAB. The propeller shaft serves as the mechanical interface between FLIGHTLAB's aerodynamic and structure representation of the rotor and the electric powertrain model in GT-SUITE. The electric powertrain model includes different components like energy sources in the form of batteries, power converters, and drives, in addition to motor controls and a mechanical representation of the propeller shaft.

To support transient dynamics, a tight coupling approach between both simulation tools was implemented. In the tightly coupled analysis, the blade-element rotor and propulsion models exchange data once per time step. A Simulink interface module was developed to pass interface data between the simulation models at each time step.

The electric propulsion model is included into Simulink by making use of a dedicated S-Function block which links directly to the GT-ISE (main modeling environment of GT-SUITE) application and allows for coupled runs between the model and Simulink. The simulation is executed from Simulink and exchanges signals in real-time in defined communication intervals, see Fig 1. The coupled simulation applications interact as follows: FLIGHTLAB provides required torque to run the propeller and propeller speed based on the flight control settings. Electrical components and system interactions are modeled in GT-SUITE to provide the power to the electric motor to match the torque and speed demands of the propeller shaft. Simulink is used to read and monitor propeller torque and speed values resulting from the aerodynamic propeller calculations in FLIGHTLAB. Simulink gains are used to match physical units of input and output data between the different interfaces. The communication interval between Simulink and GT-SUITE is set to 0.01 seconds directly from the S-Function block in SIMULINK.

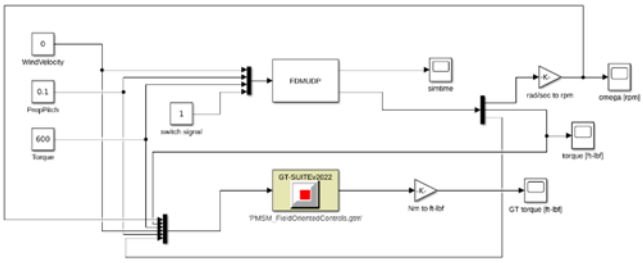

Fig. 1: Simulink Model containing FLIGHTLAB and GT interfaces

The interface module utilizes a Simulink Type 2 S-Function to pass between the blade element rotor and the electric propulsion models. the rotor real time isolated rotor model allowed for input of the electric motor torque (i.e., to drive the rotor), collective blade pitch, and a vertical airspeed component for axial climb/descent simulation. The outputs were the rotor rotational speed, shaft torque and rotor thrust, see Table 1

Table 1: Interface Parameters GT-SUITE/FLIGHTLAB

Parameter Description	Name	Unit
Input-to-FLIGHTLAB		
Wind speed, vertical	WINDZ	ft/sec
Blade collective pitch	BLADEPITCH	rad
Engine torque	ETORQUE	ft-lbf
Propulsion source switch	SWINPUT	nd
Outputs-from-FLIGHTLAB		
Rotor speed	OMEGA	rad/sec
Rotor torque, measured	HUBMZ	ft-lbf
Rotor thrust	HUBFZ	lbf

Monitors allow the transferred signals to be observed during the coupled simulation. After the simulation has completed, results of the exchanged signals can be investigated directly in Simulink. Detailed simulation results of the aerodynamic rotor load e.g., physical quantities as function of time can be accessed via the runtime operator console. Postprocessing of the drive system results is done inside the dedicated postprocessing tool GT-POST. This includes detailed time resolved plots of physical quantities of each electric powertrain component. In addition to that, the input and output signals of the FLIGHTLAB S-Function block are transferred to the GT-SUITE S-Function block to make the respective data observable in the postprocessing tool. This simplifies the postprocessing of data from various sources by creating a uniform postprocessing routine.

DEMONSTRATION MODEL DESCRIPTION

The demonstration models used in this work were based on the Uber Elevate eCRM001 configuration as described in [9]. The eCRM001 configuration shown in Fig 2 has 4 pairs of two-bladed, co-rotating coaxial lift rotors and two four-bladed cruise tilt-propellers. Note that the Uber eCRM001 configuration was also published with five-bladed cruise propellers, which were not analyzed. Fig. 2 shows the example eVTOL configuration in hover configuration as used for this initial study. In hover configuration, the cruise propellers are tilted up to provide lift. Tilting the cruise propellers forward provides horizontal thrust for low-speed and transition to cruise.

Fig. 2: Uber Elevate eCRM001 eVTOL Configuration

ROTOR MODELS

For the investigation of the coupled system, isolated rotor models of the lift and cruise propellers were developed. The lift propellers were modeled using 20 aerodynamic segments and 7 rigid structural blade segments. For this work, the NACA0012 airfoil was used for the blade airloads. A six-state Peters-He[10] finite state model was used for the dynamic induced airflow modeling. The isolated, four-bladed cruise

propeller used similar modeling options as the lift propeller model. The propulsion model was enhanced with an interface to allow for the rotor model to be driven by an external shaft torque signal provided by the drivetrain dynamic model. The Control System Graphical Editor was used to implement a model for the rotor driveshaft that allowed for both internal and external source of rotor shaft torque. The selector switch for the propulsion source is listed in Table 1 together with the interface data of the FLIGHTLAB models for the lift and cruise propellers. The models were compiled with the listed data interface to allow for coupling with the electric propulsion model and exchanging data in the Simulink simulation environment. During the compilation process, the isolated rotor models were run to steady state using the internal propulsion system. This allowed for a reduced run-up time (initialization) and smooth coupling to the external electric propulsion system.

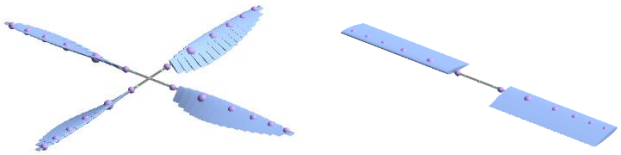

Fig. 3: FLIGHTLAB Isolated Rotor Models left cruise, right: lift

ELECTRIC POWERTRAIN MODEL

Representative, but generic, electric powertrain models for the eCRM001 lift and cruise propellers were developed to meet the rotor torque requirements and demonstrate the electric powertrain dynamics. The electric powertrain model includes different general components like energy sources in the form of batteries, power converters, drives, motor controllers, and a mechanical representation of the propeller shaft. Figure 4 shows the model map of the GT-SUITE model, demonstrating the different components and connections used to represent a fully functional electric powertrain.

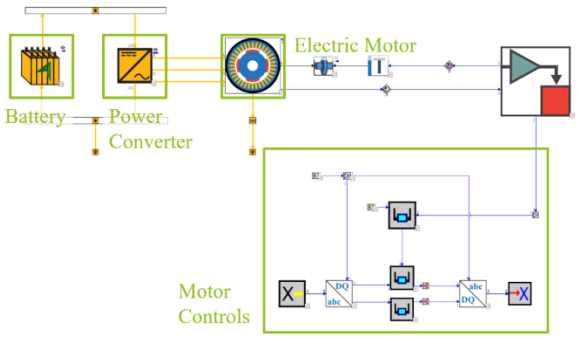

Fig. 4: Electric Powertrain and Motor Control Model in GT-ISE

The electric powertrain model allows for detailed investigations of energy consumption along the complete energy conversion path from the battery to the propeller shaft. Each component has a certain quantity of power dissipation in the form of heat which can be measured depending on the parametrization and boundary conditions of the simulation. Each component of the developed electric powertrain model is described in more detail below.

Battery: Electrochemical properties of each cell are represented by detailed physic-based models for performance and degradation of Lithium-Ion cells. The templates define a Newman Pseudo 2D (P2D) model of Lithium-ion battery cells. As illustrated in Figure 5, the different cell components are discretized in thickness direction of the cell using a finite control volume approach.

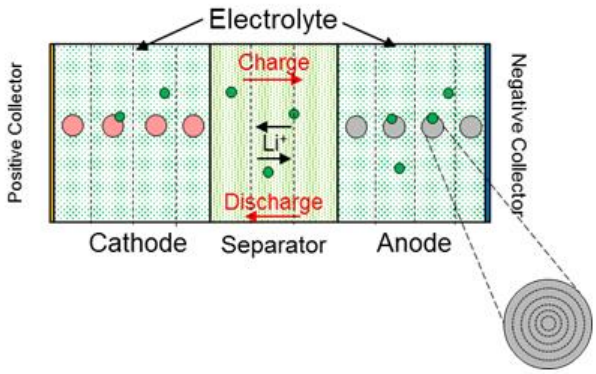

Fig. 5: Cross-Sectional representation of Pseudo-2D model of a Lithium-ion cell

The model allows simulation of the electrochemical reactions occurring inside a Lithium-ion cell by solving a set of governing equations for conservation of charge and chemical species for the solid-phase, electrolyte-phase and the active material (Eq 1-4).

$$0 = \frac{\partial}{\partial x}\left(\frac{\sigma_s \partial \phi_s}{\partial x}\right) - f^{Li} - a_{dl} C \frac{\partial(\phi_s - \phi_e)}{\partial t} \quad (1)$$

$$0 = \frac{\partial}{\partial x}\left(\kappa^{eff}\frac{\partial \phi_e}{\partial x}\right) + \frac{\partial}{\partial x}\left(\kappa_D^{eff}\frac{\partial Inc_e}{\partial x}\right) + f^{Li} + a_{dl} C \frac{\partial(\phi_s - \phi_e)}{\partial t} \quad (2)$$

$$\frac{\partial}{\partial t}[\epsilon c_s] = \frac{\partial}{\partial x}\left(D_e^{eff}\frac{\partial c_e}{\partial x}\right) + \frac{1 - t_+^0}{F} f^{Li} \quad (3)$$

$$\frac{\partial c_s}{\partial t} = \frac{1}{r^2}\frac{\partial}{\partial r}\left(D_s r^2 \frac{\partial c_s}{\partial r}\right) \quad (4)$$

Where x is the distance in the cell plane direction, t is time, σ_s is the solid phase conductivity, ϕ_s is the solid phase potential,

ϕ_e is the liquid phase potential, a_{dl} is the specific interfacial area, C is the specific capacitance, f_{Li} is the reaction current of the Lithium, κ_{eff} is the electrolyte effective ionic conductivity, κ_d^{eff} is the effective diffusional conductivity, c_e is the Li+ concentration in the electrolyte, c_s is the Li+ concentration in solid, ϵ is the porosity, D_e^{eff} is the electrolyte phase Lithium Diffusion coefficient, t_+^0 is the transference number, F is Faraday's constant and r is the particle radius.

This allows for detailed prediction of the terminal voltage, current, power, heat rejection, and amount of Lithium throughout the cell. In addition, the electrochemical models can be used to model aging mechanisms of battery cells. This is done by providing physics-based models for SEI layer growth, cathodic film layer growth, anode lithium plating, and Li+ isolation due to active material cracking. All these features allow for significant decrease of battery testing times and better understanding of battery performance and aging in real-world operating scenarios.

The electric powertrain model utilizes a NCM811 (Lithium-Nickel-Manganese-Cobalt-Oxide) chemistry for the battery active material, along with a graphite cathode material. This cell type is widely used in the automotive industry and is known for providing high energy densities. The battery pack for the proposed eVTOL configuration includes a total of 3200 cylindrical cells (80 series, 40 parallel). The temperature of the battery pack is calculated from the heat generated from electrochemical reactions, resistive losses, and entropic heating.

Power Converter: An efficiency-map based inverter is used to transform the DC electrical quantities from the battery pack into 3 phase electrical quantities which can be used to drive an electric machine. The efficiency map is implemented as a function of DC voltage and temperature. The inverter produces dissipating heat depending on the inverter efficiency under the current operating conditions.

Electric motor: A detailed electric machine model is used to transform the electrical power provided by the battery pack into mechanical power driving the propeller shaft. The electric machine is represented by a detailed electrical equivalent circuit modeling a Permanent Magnet Synchronous Machine.

Motor Controls: A model-based controller creates the 3 phase voltage commands imposed to the electric machine by the power converter (inverter). The controller uses information about the electric machine and its operating conditions to create 3 phase voltage signals based on a torque target for the electric machine.

The motor controller takes the propeller speed as a target speed and creates AC voltage signals for the motor to reach the speed target. The controller is divided into two main stages and uses Park-Clarke-Transformation algorithms to transform the three phase AC voltage and current signals into the rotating d-q-reference frame [11]. The first controller stage uses electric machine speed as control variable, whereas the controller output is used as q-current. While this signal is used as the target signal for the q-current controller within the second stage of the motor controls, the d-current controller is constantly targeting a zero d-current. Outputs of the d- and q-current controllers are interpreted as d- and q- voltages respectively. These signals are fed through an inverse Park-Clarke-Transformation algorithm creating AC-Voltage signals which can be imposed onto the windings of the electric machine. The current load resulting from applied voltage and motor resistance (stator and induced resistance) acts on the battery and results in a decrease of SOC (State of Charge) of the battery cells.

ELECTRIC POWERTRAIN SIZING

The performance characteristics of the eCRM001 electric powertrain components were not known from web sources or literature. Therefore, a trim analysis of the rotor models was performed, to calculate operating limits of the electromechanical interface. The trimmed rotor torque and speeds in steady flight were used to find a suitable electric powertrain configuration for the given operating conditions.

The electric motor model was initially parametrized from an existing automotive application and sized up to match the torque and speed demands of the eCRM001 lift and cruise propellers. Both a speed controller and a model-based torque controller were used for initial tests to ensure the motor performance. Performance relevant motor parameters listed below were adjusted based on the eCRM001 power requirements:

- Stator Resistance
- Number of Poles
- Magnet Remanence
- Magnet Flux Linkage
- D- and q-axis Inductances

The size of the proposed battery pack was chosen to support the electrical load of the motor at the required eCRM001 operating conditions. The battery pack has a sufficient size for both steady state and transient tests at the operating conditions of the electric powertrain.

DEMONSTRATION RESULTS

Several tests utilizing the integrated simulation framework have been performed. Both the lift and cruise propeller models were used to investigate the coupled system interactions and effects on the electric powertrain model. The test cases were selected to resemble real-world operating conditions and to investigate the importance of the combined simulation framework and the electric powertrain performance.

SIZING OF ELECTRIC POWERTRAIN COMPONENTS

The first tests of the coupled simulation framework were performed on an isolated model of the lift propeller. By applying a torque step function input to the isolated rotor model block in Simulink the resulting torque and speed signal of the propeller were transferred to the electric propulsion model. Figure 6 shows the commanded rotor torque and the applied rotor torque in the rotor model. The results of those tests shown in Figures 7,8 confirm the appropriate sizing of the e-machine by demonstrating that the motor can sufficiently match the speed and torque targets provided by FLIGHTLAB. The transient from 0-5 seconds is due to initial synchronization between both simulation models and is also noticeable for the other results shown in this section.

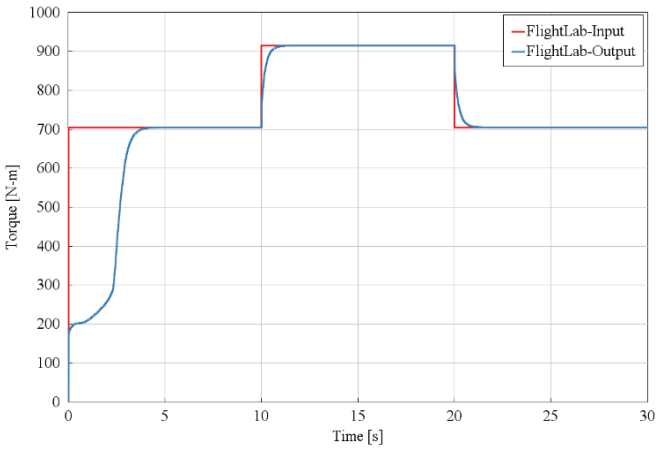

Fig. 6: Lift-Propeller model: Input and Output Torque Signals

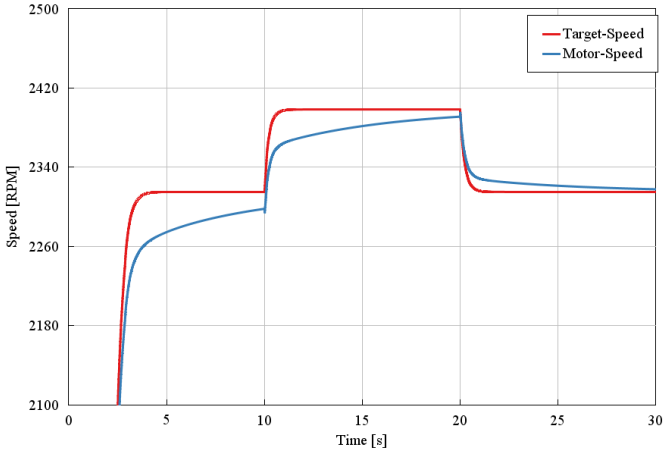

Fig. 7: Lift-Propeller model: Input and Output Torque Signals

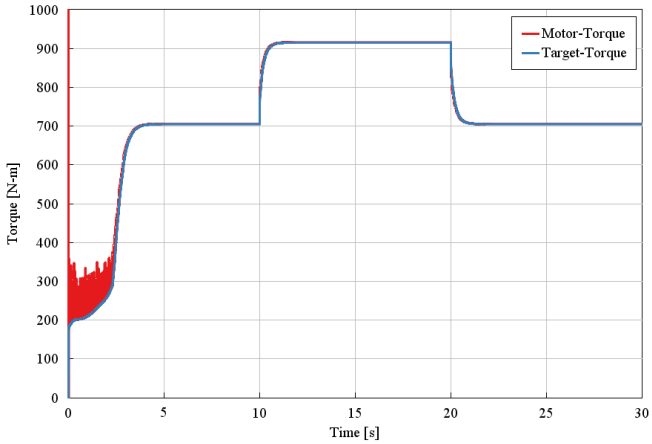

Fig. 8: Comparison of Rotor Hub Torque calculated by FLIGHTLAB and Motor Torque

SINUSOIDAL AND REPEATING SQUARE TORQUE SIGNALS

The lift propeller thrust was controlled by changing the propeller speed at a fixed collective pitch angle of the propeller blades. Various tests were performed on the combined system model to evaluate the behavior of the electric powertrain at different loads on the lift propeller.

Sinusoidal and repeating square functions of torque over time were imposed on the lift propeller. While in a hover, the lift propellers were controlled to maintain a constant velocity and provide a constant lift force resulting in zero vertical acceleration. The main objective of these tests was to resemble speed variations of the lift propellers controlled by a flight control system during unsteady wind conditions. The inputs and outputs of the rotor model itself were compared to investigate the offset between engine torque acting on the propeller and the resulting rotor torque of the blade element model in FLIGHTLAB. Figures 9 and 10 show the sinusoidal and square functions of torque imposed onto the motor shaft inside the electric powertrain model response with the measured torque.

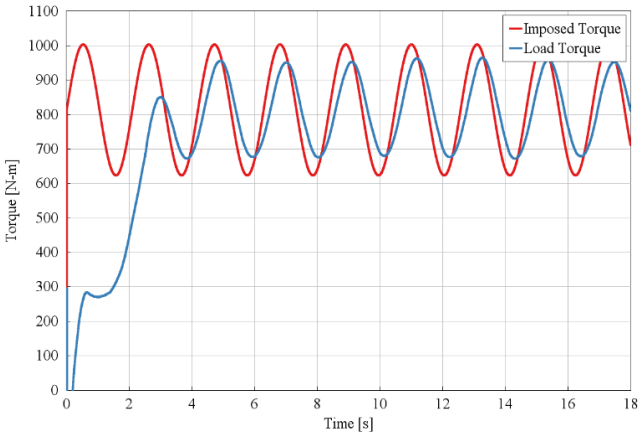

Fig. 9: Lift-Propeller Model: Input and Output Torque Signals at Sinusoidal Excitation

Both sinusoidal and repeating square inputs show deviations between applied and rotor hub torque during the initial run up of the dynamic simulation. In addition to that, both inputs show a significant delay in measured rotor hub torque peaks because of the propeller moment of inertia. These results can be especially useful for further controller design and tuning of flight control system for a complete airframe model.

Further, the e-powertrain model allows investigation of the impact of sinusoidal and repeating square torque excitations on the electric powertrain components. The electric motor must provide the necessary mechanical power to counteract the rotor hub torque while running the propeller at the given speed. While the electric motor provides the necessary mechanical power, it draws electrical power in the form of voltage and current from the electrical circuit. The electric powertrain model enables simulation of the complete power conversion from the battery pack to the propeller shaft, while taking conversion efficiencies of the different components into account.

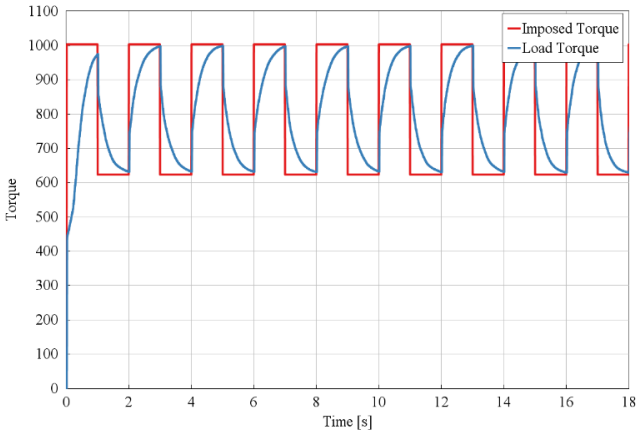

Fig. 10: Lift-Propeller Model: Input and Output Torque Signals at Repeating Square Excitation

Therefore, the coupled simulation framework allows for direct investigations of the effect of sinusoidal and repeating square torque signals on battery degradation. Figure 11 compares the impact of both torque inputs on battery performance in terms of battery SOC (State-of-Charge). Note the initial charge shown in Figure 11 is less than one because the simulation was run to steady state prior to recording the SOC time history.

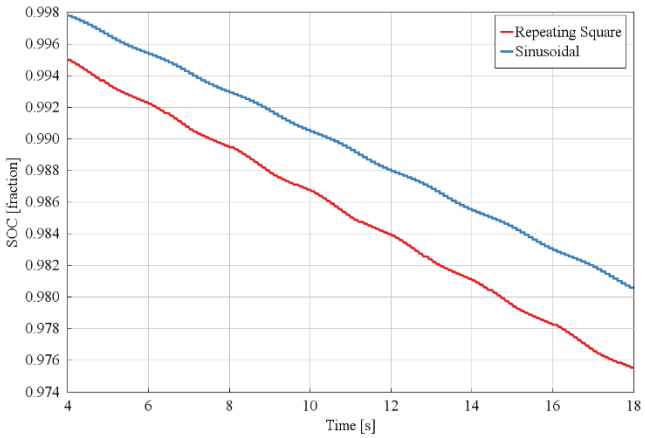

Fig. 11: Impact of Sinusoidal and Repeating Square Torque Targets on Battery State-Of-Charge (SOC)

The repeating square function comes with higher gradients in rotor hub torque. This requires more current draw from the battery to make the motor follow the dynamically changing torque load and results in higher SOC gradients. As a result, the SOC of the battery pack decreases faster for the square wave torque load than for the sinusoidal torque load, even though the effective torque amplitude is similar for both signals.

In addition to general performance characteristics, the battery template allows for thermal analysis of the battery pack. Figure 12 shows the heat rate generated by the described battery pack for both sinusoidal and repeating square excitations. Besides faster SOC degradation, the higher load current of the repeating square excitation results in higher heat rates generated by the battery pack, which also affects the battery performance.

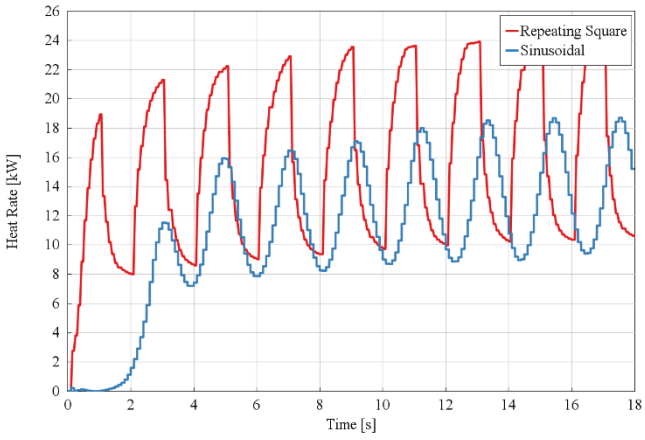

Fig. 12: Impact of Sinusoidal and Repeating Square Torque Targets on Heat Generation Rate of Battery Pack

VERTICAL WIND VELOCITY ON LIFT-PROPELLER

The lift propellers and electric powertrain components must be able to satisfy mission requirements for hover and climb maneuvers of the rotorcraft. A typical trajectory of an eVTOL starts with a vertical climb until a specific travel altitude is reached. This climb at a positive vertical velocity creates a relative wind velocity acting on each of the lift propellers. This velocity component acts as an axial flow on the lift propeller, assuming a vertical climb with no velocity components in the longitudinal or lateral directions. This relative wind velocity acting on the lift propeller during climb can be imposed to the isolated rotor model via an input signal port on the FLIGHTLAB S-Function block. Figure 13 shows the imposed vertical velocity and the effects on rotor hub torque and propeller speed, calculated by the FLIGHTLAB model of the lift propeller. The wind is acting as a downwash on the lift propeller, while a constant engine torque is imposed on the propeller.

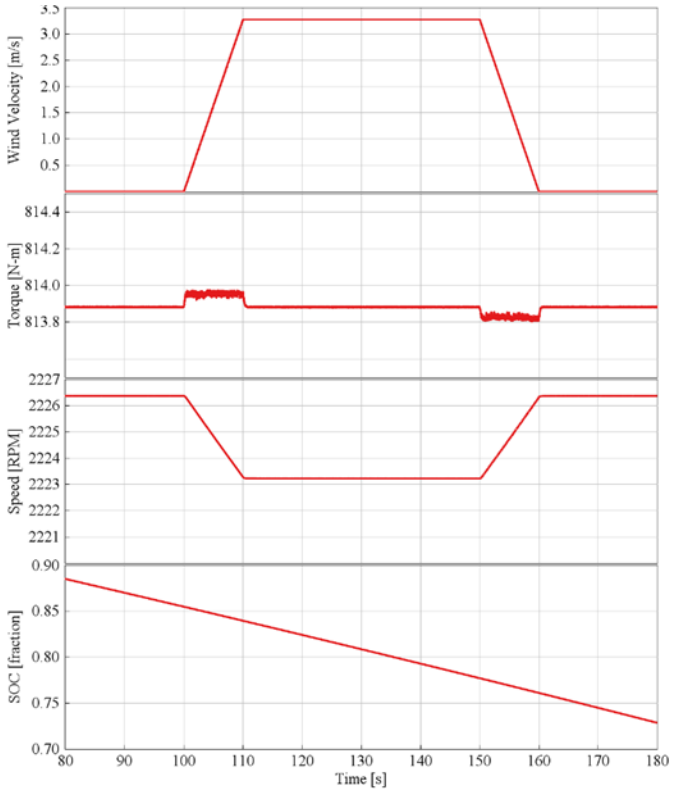

Fig. 13: Lift-Propeller model: Impact of nonzero Wind-Velocity on Propeller Speed, Rotor Hub Torque and Battery SOC

In this test the motor controller held a near constant torque and allowed the rotor speed to change. The nonzero vertical wind velocity had little to no visible impact on the battery performance, whereas the speed of the propeller changed slightly with the relative wind velocity changes.

EFFECT OF BATTERY SOC ON MOTOR PERFORMANCE/PROPELLER SPEED

The duration of the coupled simulation was increased to show the effects of long duration operation of the electric powertrain. The target of this test was to show propeller speed limits, caused by limitations of the electrical components. The lift propellers run at very high speeds and torques which can create testing conditions at the limits of the electric powertrain component capabilities. One significant limiting factor of the proposed electric powertrain architecture is the SOC of the battery pack. As the SOC decreases, the open-circuit-voltage of each individual cell decreases, resulting in a lower effective voltage of the complete battery pack. Keeping the target speed and blade pitch constant, means that the motor must be provided with a constant power source over the simulation duration. With lower DC voltage provided by the battery, the motor must draw a higher DC current from the battery. This results in faster SOC degradation and can even result in exceeding the C-Rate limits of the battery pack. The C-Rate is used to classify charge and discharge currents of a battery pack and is the ratio of the load current to the battery capacity. For the sake of this test case, a maximum battery current of 780A was chosen, which is equal to a maximum C-Rate of ~6C.

To account for this limit in the existing control strategy, the output of the motor controller has to be restricted. Since the d-Current Id is always controlled to be zero, the maximum operating speed is limited by the amount of q-voltage imposed to the machine. In order to impose this limitation, the q-voltage Vq has to be calculated from the current operating voltage of the battery pack and the DC current limit of the battery. The three-phase instantaneous power P_{batt} in terms of d-q-0 quantities is described by the following equation [12]:

$$P_{batt} = \frac{3}{2}\left(V_d I_d + V_q I_q + 2V_0 I_0\right) \tag{5}$$

With all quantities being described in SI-Units (Power: [W], Current: [A] and Voltage: [V]). Since d-current I_d and voltage V_0 are controlled to be zero by the implemented control strategy, Equation 1 simplifies to:

$$P_{batt} = \frac{3}{2} V_q I_q \tag{6}$$

The battery voltage decreases with SOC degradation of the battery cells. The load current on the battery pack should be limited to 780A as explained above. These assumptions allow calculation of the q-voltage limit $V_{q\text{-limit}}$ as a function of the battery voltage U_{batt}, battery current $_{Ibatt,}$ and q-current I_q:

$$V_{q-limit} = \frac{2U_{batt} * I_{batt}}{3I_q} \quad (7)$$

This equation was added to the motor control strategy and was used to overwrite the maximum output limit of the q-current controller at every timestep of the coupled simulation. The battery effective voltage U_{batt} was sensed from the battery pack at every timestep and the battery load current I_{batt} was set to 780A as described above. This ensured that the AC voltages imposed to the electric motor did not result in DC currents exceeding the defined limit.

While the effective DC voltage provided by the battery pack decreases with SOC degradation, the q-current imposed by the control strategy increases up to its maximum limit. Once the controller output hits the limit calculated by Equation 3, the q-current imposed on the electric machine windings stays constant at the maximum value, assuming load torque and speed target stay constant as well. With the battery volage decreasing and the DC current being limited to 780A, the speed of the motor will decrease as the battery SOC decreases further. Figure 14 shows the results of a transient analysis of machine speed. Figure 15 shows the q-current controller performance.

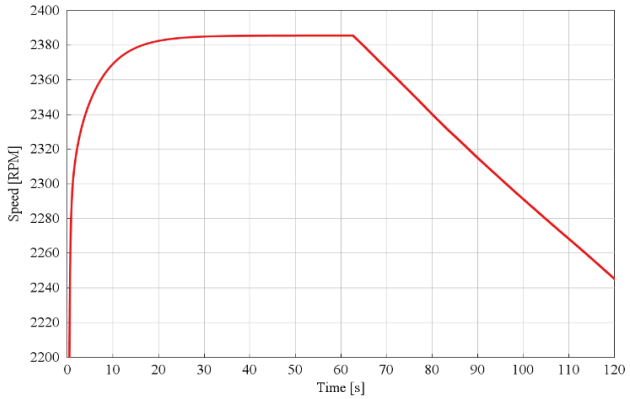

Fig. 14: Effect of Battery SOC Degradation on Propeller Speed

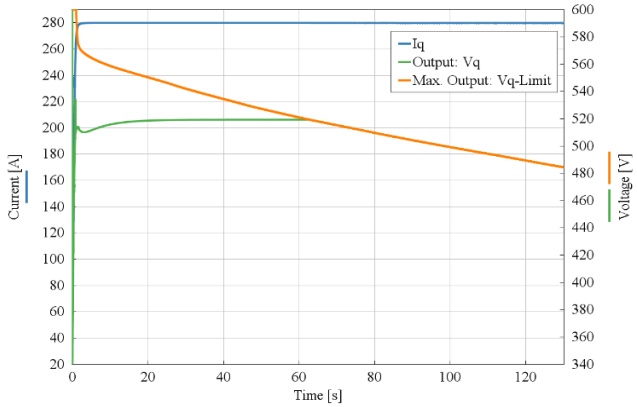

Fig. 15: Effect of q-Voltage Limitations due to Battery SOC Degradation on Motor-Controller Performance

As soon as the controller output hits the maximum limit, Figure 14 shows the machine speed decreasing. This occurs at a SOC level of ~88%.

While this is an exemplary study highlighting the capabilities of the coupled simulation framework, the SOC gradients of the battery pack will differ from the physical configuration due to differences in battery pack size and electric machine design. Nevertheless, this study highlights the importance of the proposed integrated simulation framework in order to find the best system design in terms of power consumption. Since the speed decrease shown in Figures 14 and 15 leads to decreased thrust generated by the lift propellers, this system behavior can be critical to system and passenger safety.

Possible countermeasures to avoid decrease in propeller speed are to increase the allowed current load on the battery pack or to increase the battery pack size by adding more cells.

CHEMISTRY VARIATIONS

An important battery performance factor is the electrolyte chemistry and the separator material. In the GT-SUITE electric powertrain model it is possible to quickly switch between different industry-relevant electrolyte chemistries. This is an important feature to decide on the best performing battery pack for a specific application.

eVTOL applications require a high power-density battery pack since weight is one of the most crucial factors in a rotorcraft's design. In addition to detailed electrochemical design, the battery pack template in GT-SUITE includes a preprocessing feature to calculate the weight of each battery cell and the complete battery pack based on used materials and cell layout. Together with the detailed performance characteristics, this modeling approach allows for detailed evaluations of different battery chemistries taking battery weight into account.

To demonstrate the importance of this type of case study, a comparison of two different battery chemistries was performed with the coupled simulation model of the lift propeller in a hover state. Along with the previously used NCM811 electrolyte chemistry, LFPO (Lithium-Iron-Phosphate) was chosen as the second electrolyte chemistry.

The following a study compares the NCM811 battery pack with a LFPO battery pack of the same total pack weight. The NCM811 battery pack is built from 3200 identical cylindrical cells. The LFPO cell is a bit lighter which increases the LFPO battery pack size to 3300 in order to match the same total pack weight of the NCM811 pack. Fig. 16 shows Open-Circuit-Voltages (OCVs) of single cells of both chemistries.

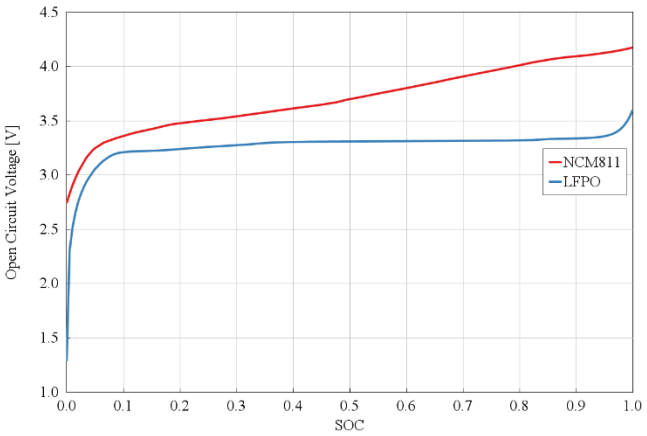

Fig. 16: Open-Circuit-Voltage Comparison of Single NCM811 and LFPO Battery Cells

The NCM811 cell shows higher OCV values over SOC. While the NCM811 cells OCV decreases over SOC degradation, the LFPO cells characteristic shows a plateau at around 3.3 Volts where a nearly constant OCV value is maintained over a large SOC range. The OCV of a single cell determines the effective operating voltages of the complete battery pack. While the number of parallel cells determines the effective capacity of the battery and the speed of SOC degradation at a constant electrical load, the number of series cells determines the effective operating voltage of the pack. Since the supply voltage of the electric motor determines the maximum speed of the machine, the series/parallel layout of the LFPO battery pack was adjusted to match the operating range of the NCM811 pack in terms of operating voltage. The NCM811 cell series/parallel layout was 80/40 while the LFPO cell layout was 100/33. Fig. 17 shows the resulting OCV characteristic of both complete battery packs after assembly.

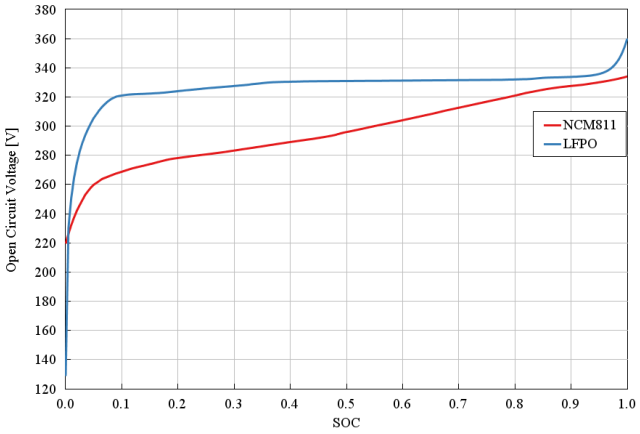

Fig. 17: Open-Circuit-Voltage Comparison of NCM811 and LFPO Battery Packs

With the modification of pack layout, an increased OCV of the LFPO battery pack was achieved. This modification ensures that the LFPO battery pack is able to support the same voltage and current loads as the previously used NCM811 cell.

As explained above, the lift propeller model was chosen to evaluate the battery pack performance. A steady hover maneuver was simulated by imposing a constant engine torque on the FLIGHTLAB model resulting in constant propeller speeds. Both simulations were run with a high maximum runtime to allow comparison of general SOC degradation and the duration the propeller was maintained at the targeted speed. Fig. 18 shows the comparison of SOC degradation of both battery packs at identical operating conditions and therefore identical electrical loads imposed on the batteries by the connected electrical components.

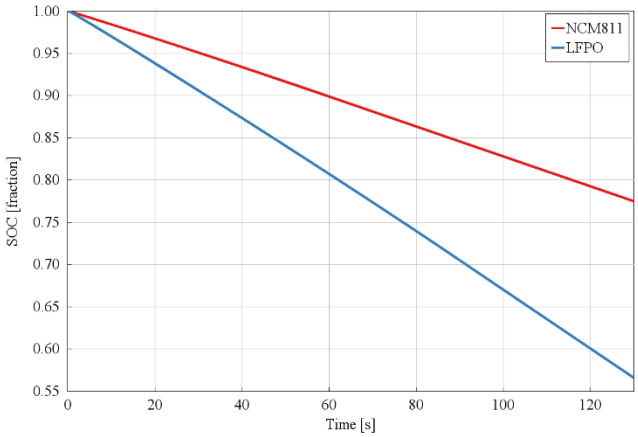

Fig. 18: Effect of Chemistry Variation on Battery Pack Performance (SOC)

The NCM811 pack shows significant slower SOC degradation over the LFPO chemistry at similar battery pack weights.

Figure 19 shows a speed comparison of the electric motor using the NCM811 and LFPO battery packs.

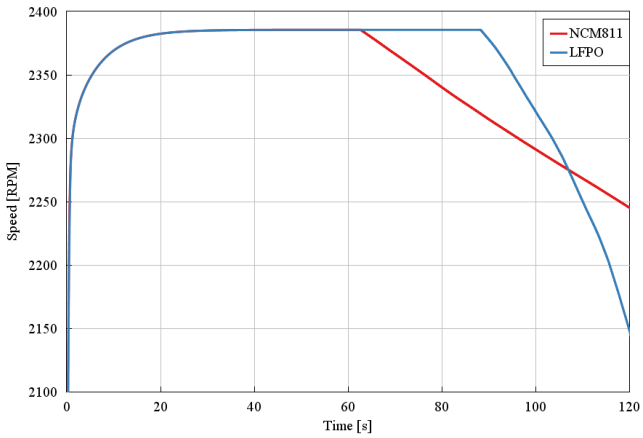

Fig. 19: Effect of Battery Chemistry Variation on Propeller Speed

When using the NCM811 cell, the motor speed decreases at an earlier stage of the simulation compared to the simulation model using the LFPO cell configuration. This behavior was caused by the shape of the OCV curves shown in Fig. 16 and 17. While the OCV of the NCM811 cell constantly decreases

over SOC degradation, the LFPO pack was able to maintain a certain operating voltage over a wider SOC range. As soon as the battery is not able to provide enough voltage to the electric motor to maintain the target speed, the speed of the propeller decreases. For the NCM811 cell this happens early, at a SOC of approx. 88%. The LFPO battery pack was able to provide enough voltage to maintain the target speed until a SOC of around 71%.

CONCLUSIONS

The coupling of FLIGHTLAB and GT-SUITE was successfully demonstrated in this paper and enables detailed analysis of the electric propulsion system under dynamically changing rotor load conditions. The combined dynamic system may be needed for analysis of transient maneuvers where the rotor dynamic load requirements may exceed the capability of individual components in the electric propulsion system.

The initial coupling results showed that the electric powertrain components were able to provide the necessary mechanical power to drive the eCRM001 lift and cruise propeller models. Multiple test cases demonstrated the integrated simulation framework under various operating conditions. Sinusoidal and repeating square wave torque signals were applied to show the lift propeller reaction in the form of rotor hub torque and the impact on the state of charge and generated heat rate of the battery pack. Small adjustments to the motor control strategies were made to limit the current load imposed on the battery pack to ensure battery safety. Results showed significant dependency of propeller speed on battery SOC for longer operations. In addition, the effects of external wind velocities on the lift propellers and the variations of battery electrolyte chemistries on the performance of the integrated system were demonstrated. Changes to the electrolyte chemistry of were shown to have significant impact on the battery performance in terms of SOC degradation and therefore the effective range of a complete eVTOL configuration.

Further testing and development of the coupled analysis capability is planned for evaluation of the full vehicle Uber Elevate eCRM001 eVTOL configuration. Using an autopilot model, the full model will be flown through several maneuvers challenging the individual components of the electric propulsion system in terms of battery discharge rates, power conversion and transmission as well as heat generation and dissipation. Flight maneuvers for future work will include regular operational transient maneuvers (acceleration, deceleration, climb, turn, and short-term control inputs), aggressive avoidance maneuvers, as well as station keeping within a turbulent airwake of a landing spot. Future work may also include elastic structures. The goal of future work is to develop and provide multidisciplinary simulation tools for the eVTOL designer and operator.

Author contact:

Felix Brenner f.brenner@gtisoft.com,

Jan Goericke jan.goericke@flightlab.com,

Matt Hasbun matt.hasbun@flightlab.com.

Llorenc Foraste Gomez ll.foraste@gmail.com

REFERENCES

1. Roper, J; “The technical challenges still to be solved before eVTOLs can become air taxis”, Aerospace Testing International, May 2021
2. Podlaski, M., Niemiec, R., Vanfretti, L., and Gandhi, F., "Multi-Domain Electric Drivetrain Modeling for UAMScale eVTOL Aircraft ," Proceedings of the 77th Vertical Flight Society Annual Forum, Virtual, May 10–14, 2021.
3. Lombaerts, Thomas & Kaneshige, John & Schuet, Stefan & Aponso, Bimal & Shish, Kimberlee & Hardy, Gordon. (2020). Dynamic Inversion based Full Envelope Flight Control for an eVTOL Vehicle using a Unified 8 Framework. 10.2514/6.2020-1619
4. Shi, X. “Intelligent Control for Fixed-Wing eVTOL Aircraft” Doctoral Thesis, California Institute of Technology, January 2021
5. Zart, N; “The Airbus Vahana Flies”, CleanTechnica Online Journal, October 2019
6. Du Val, R. W., He, C. “Validation of the FLIGHTLAB virtual engineering toolset,” The Aeronautical Journal, Volume 122, No 1250, April 2018
7. Harrison, J; Devin, C; Zenker, J; Frank, E.; “Using Multi-Physics Simulation to Predict Battery Pack Thermal Performance and Risk of Thermal Runaway During eVTOL Aircraft Operations” AIAA Propulsion and Energy 2019 Forum August 2018 https://doi.org/10.2514/6.2019-4406
8. Foraste Gomez,L; Brenner, F; Huang, Z; “Integrated Multi-Physics Simulation for eVTOL In-flight Energy Regeneration using Piezoaeroelastic Power Harvesters and 6DOF Control” Vertical Flight Society Forum 78, May 2021
9. Kim, J., He, C., Goericke, J., “Modeling and Analysis of eVTOL Air Vehicle Interactional Aerodynamics and Mission Performance,” VFS Aeromechanics for Advanced Vertical Flight Technical Meeting, San Jose, CA, January 2123, 2020
10. Peters, D., He, C., “A finite-state induced-flow model for rotors in hover and forward flight,” 43rd Annual National Forum of the American Helicopter Society, St. Louis, MO, May 1987.

11. Bhangu, B., Bingham, C. “Nonlinear State-Observer Techniques for Sensorless Control of Automotive PMSM’s, including Load-Torque Estimation and Saliency”, EPE Toulouse, France 10th European Conference on Power Electronics and Applications 2003
12. Akagi, H., Ogasawara S., Kim, H. “The theory of instantaneous power in three-phase four-wire systems: a comprehensive approach”, Okayama University 1999
13. He, C.; and Zhao, J. “Rotor Wake Dynamics with Viscous Vortex Particle Method” AIAA Journal 2009 47:4, 902-915